Article:
Bradley, D and Shehata, M (2018) Acceleration of laminar hydrogen/oxygen flames in a tube and the possible onset of detonation. International Journal of Hydrogen Energy, 43 (13). pp. 6734-6744. ISSN: 0360-3199

https://doi.org/10.1016/j.ijhydene.2018.02.068

Acceleration of Laminar Hydrogen/Oxygen Flames in a Tube and the Possible Onset of Detonation

D. Bradley* and M. Shehata

School of Mechanical Engineering, University of Leeds, Leeds LS2 9JT, United Kingdom

*Corresponding author

*e-mail address: d.bradley@leeds.ac.uk

Abstract

The possibility is analysed of a laminar flame accelerating along a cylindrical tube, closed at one end, and inducing a deflagration to detonation transition in a stoichiometric H_2/O_2 mixture. The pressure and temperature ratios at the ensuing shock wave increase, as do laminar burning velocities, while autoignition delay times decrease. Combined with appreciable elongation of the flame, these enhance the strength of the shock. The conditions necessary for delay times of 0.05, 0.1, 1.0 and 5.0 ms, at an unburned mixture critical Reynolds number of 2300, are computed for different tube diameters. Probable consequences of the different delay times and hot spot reactivity gradients, including detonation, are all considered. The probability of a purely laminar propagation leading to a detonation is marginal. Only when the initial temperature is raised to 375 K, do purely laminar detonations become possible in tubes of between about 0.5 and 1.35 mm diameter.

Key words

Laminar burning velocity, Autoignition delay time, DDT, Detonation peninsula, Excitation time

Nomenclature

A	flame surface area associated with u_t (m^2)
a	cross section area of tube and sound speed (m^2, m/s)
a_1	acoustic velocity ahead of the shock (m/s)
c	a defining parameter for M_1 see Eq. (8)
D	tube diameter (mm)
D_c	critical tube diameter for laminar flow (mm)
E	activation energy (J mol^{-1})
$\bar{E}$	detonation stability dimensionless group
K, K_s	Karlovitz stretch factor
K_{ql+}	laminar extinction Karlovitz stretch factor
M_1	Mach number of shock wave
P_0	reference pressure (MPa)
P_1	shock wave upstream pressure (MPa)
P_2	shock wave downstream pressure (MPa)
	tube radius and hotspot radius (mm)
Re_c	critical Reynolds number
$\bar{r}$	normalised hotspot radius
S_f	flame speed along tube (m/s)
S_g	mean gas velocity ahead of flame (m/s)
S_h	shock wave speed along the tube (m/s)
T_0	reference temperature (K)
T_1	shock wave upstream temperature (K)
T_2	shock wave downstream temperature (K)
u	flow velocity (m/s)
u_a	autoignition propagation velocity (m/s)
u_ℓ	laminar burning velocity (m/s)
u_t	turbulent burning velocity (m/s)

Greek

α , β	numerical constants
γ	ratio of specific heats
ρ_b	burned gas density (kg/m^3)
ρ_u	unburned gas density (kg/m^3)
σ	density ratio ρ_u/ρ_b
ν	kinematic viscosity (m^2/s)
τ_i	ignition delay time (s)
τ_e	excitation time (s)
ξ	a/u_a
ε	residence time of pressure wave in hot spot normalised by excitation time

Suffices

c	critical value
m	maximum value

1. Introduction

The deflagration to detonation transition, DDT, arises from a flame propagating in a duct when the burning velocity is sufficiently high to create a shock wave that is strong enough to trigger autoignition. The heat release from this that feeds into the pressure wave created by the originating rate of change of heat release rate, may be sufficient to create a detonation. Usually the combustion is turbulent and the turbulent feed-back mechanism accelerates the flame to a sufficient extent before further turbulence leads to a decline in the turbulent burning velocity and ultimate flame quenching [1]. It is an important explosion hazard, a desirable phenomenon in detonation engines, and an undesirable one in more conventional internal combustion engines [2]. In the case of very reactive mixtures, such as stoichiometric H_2/O_2, it might be possible to attain a sufficiently high laminar burning velocity for the attainment of autoignition, without further supplementing the burning rate with generated turbulence, but this is unclear.

Interestingly, evidence as to whether such a laminar transition is possible has not been clearly demonstrated experimentally. It is unclear whether both the burning velocity of stoichiometric H_2/O_2 and the flame front area can be sufficiently high, whilst the tube diameter might have to be so small to maintain laminar flow that the associated stretch rate and heat loss would extinguish the flame. Quantitatively, study of this possibility is not helped by the confusing spread, over orders of magnitude, of both measured and chemical kinetically modelled values of ignition delay times, τ_i, at different pressures and temperatures, and, to a lesser extent, the values of laminar burning velocity, u_ℓ. The purpose of the present paper is to review the associated data for all these parameters, endeavouring to reduce uncertainties, in an examination of the conditions that might make a laminar detonation of stoichiometric H_2/O_2 possible.

Usually laminar burning velocities are insufficient to generate a shock waves strong enough to autoignite the mixture ahead of the flame, and DDTs occur more readily with turbulent flames. To generate a rapid DDT, turbulence has been created by roughened tubes which have an enhancing effect on flame propagation, due to the induced flame wrinkling [3-6]. In addition, the use of restrictive obstacles was pioneered by Chapman and Wheeler [7] who increased the flame speed by inserting rings. Subsequently, Shchelkin [8, 9], introduced a spiral coil inside the tube, which very effectively shortened the run-up distance to DDT, a particularly important consideration in detonation engines. Such coils develop vortices and generate turbulence, with more rapid acceleration of the flame.

In contrast, many experimental [10-17] and numerical studies [14, 18-23] have analysed DDT in a smooth duct. Urtiew and Oppenheim [10] conducted DDT studies with reactive mixture, of equi-molar and stoichiometric H_2/O_2 in a rectangular smooth duct, 3.81 x 2.54 cm, closed at one end. They photographically recorded the "explosion within the explosion", attributed to the interaction of the flame with the walls of the tube. A train of compression waves created from this interaction indicated a DDT, developing between the turbulent flame front and shock wave. A "strong ignition" was characterised by low values of $\partial\tau_i/\partial T$ by Meyer and Oppenheim [17].

Kuzentsov et al. [11] exploded stoichiometric H_2/O_2 mixtures in a smooth tube, at different initial pressures ranging from 0.02 to 0.8 MPa, and suggested that a growing turbulent boundary layer controlled the turbulence and the onset of DDT. High shear rates can be generated in viscous sub-layers, which might initiate autoignition, aided by weak transverse waves from hot spots [24].

Liberman and co-workers suggested that in such highly reactive mixtures, as stoichiometric H_2/O_2, ethylene/oxygen and acetylene/oxygen, the DDT could be triggered by laminar combustion [12-14, 19], while for less reactive mixtures, such as those of methane-air, turbulence was necessary [25]. In their experimental studies of stoichiometric H_2/O_2, Kuznetsov et al. [12] and Liberman et al. [13] suggested it was uncertain whether a DDT followed the Zel'dovich reactivity gradient mechanism, developing at hot spots in the unreacted mixture ahead of the flame.

Liberman et al. [13], in their studies of DDTs of stoichiometric H_2/O_2 and ethylene/oxygen mixtures considered the upstream flow to remain laminar up to the transition to detonation. In experiments with stoichiometric H_2/O_2, in a duct of 50 x 50 mm cross section, Kuznetsov et al. [12] reported the flow ahead of the flame remained laminar in the bulk. Furthermore, in their 3D computational study of the DDT of stoichiometric H_2/O_2 at 298 K and 0.1 MPa, in a duct of 10 x 10 mm cross-section, Ivanov et al. [19] wrote that "the flow remains laminar everywhere in the channel ahead of the flame all the time till the transition to detonation.'' Optical imaging suggested the onset of a turbulent flame pattern at the transition. Here the problem is whether a configuration that requires a high flow velocity to create strong enough shock waves, can maintain laminar flow with practical duct sizes.

The high reactivity of such mixtures, particularly at low pressure, suggests transitions to detonation may not require significant turbulence to accelerate the flame. In their experimental study with stoichiometric ethylene/oxygen in micro tubes of 0.5, 1 and 2 mm diameter at 0.1 MPa, Wu et al. [16] observed, for the first time, transition to detonation in micro-tubes. Laminar flame accelerations were very rapid and values of Reynolds number suggested that the initial flame became turbulent.

In the absence of flame wrinkling due to turbulence, a key factor in the flame acceleration, is the elongated parabolic gas velocity distribution ahead of a laminar flame. This increases the ratio of flame area, A, to that of the cross-sectional area of flow, a. In a numerical study of laminar flame propagation in stoichiometric acetylene-oxygen mixtures in a narrow channel with adiabatic walls, Gamezo and Oran [26] showed that high values of A/a were rapidly attained, in the absence of strong shock. The relatively rapid attainment of high velocities ahead of the flame is a valuable characteristic for micro-propulsion devices. Even with intense turbulence, the generation of DDTs with CH_4/air can only be achieved with large diameter tubes [27, 28].

The present paper analyses whether the gas flow created by stoichiometric H_2/O_2 laminar flames can create sufficiently strong shock waves to autoignite the mixture. This requires comprehensive data on τ_i, and burning velocities, u_ℓ. The analysis is based on that for a one dimensional DDT, as in [1], and indicated by Fig. 1, with an accelerating flame creating an ever-stronger shock wave. Major factors for the attainment of laminar flow DDT are low values of τ_i, combined with high values of u_ℓ and kinematic viscosity, ν. This schematic diagram depicts the propagation of the flame from the closed end of a duct, generating a shock wave ahead of it.

2. Analysis

Fig. 1: Flame and shockwave propagation in an open ended tube. Ignition initiated from the closed end [1].

The analytical approach requires a detailed knowledge of u_ℓ of the mixture, as well as of τ_i, both at high temperatures and pressures. Limitations of the approach are the one dimensionality, incomplete and insufficiently accurate data on u_ℓ and τ_i, and no allowance for transverse weak shock waves. The procedure is to identify the conditions necessary to generate particular values of τ_i. The different modes of autoignition are discussed in Section 7.

In [1] it is shown that the flame speed in the duct is given by

$$S_f = (A/a)\sigma u_\ell, \qquad (1)$$

in which A is the laminar flame surface area, a the cross sectional area of the duct, and σ the ratio of unburned to burned gas density. The gas velocity ahead of the flame, towards the shock, S_g, is given by

$$S_g = (A/a)(\sigma - 1)u_\ell. \quad (2)$$

Close to the shock wave, if S_h is the shock wave speed along the duct, and u_2, the gas velocity relative to the shock wave, away from it and towards the flame, then,

$$S_g = S_h - u_2. \quad (3)$$

The increased temperature and pressure due to the confinement and shock increase u_ℓ, which also elongates the flame area, both of which further increase S_g and strengthen the shock.

It is assumed that there is no gas velocity just ahead of the shock wave, where conditions of the unburned gas are designated by the suffix 1. The unburned gas velocity, u_1, into the shock wave, and relative to it, must be equal to S_h.

The shock wave equations [1] give the ratio of velocities into and out of the planar shock wave as:

$$\frac{u_2}{u_1} = \frac{2+(\gamma-1)M_1^2}{(\gamma+1)M_1^2}. \quad (4)$$

Here M_1 is the Mach number associated with the speed of the shock wave along the duct, given by u_1/a_1, with a_1, the acoustic velocity ahead of the shock.

Equation (3), with $S_h = u_1$, yields:

$$S_g/u_1 = 1 - u_2/u_1\ , \quad (5)$$

which, with Eq. (4), gives

$$S_g = \frac{2(M_1^2-1)a_1}{(\gamma+1)M_1}. \quad (6)$$

Equations (2) and (6) give a quadratic equation in M_1 with a real solution:

$$M_1 = (c/2) + (1 + c^2/4)^{1/2}, \text{ where} \quad (7)$$

$$c = (S_g/a_1)(\gamma + 1)/2 = (A/a)\, u_\ell(\sigma - 1)\left(\frac{\gamma+1}{2a_1}\right). \quad (8)$$

The pressure and temperature ratios at the planar shock wave are given by:

$$\frac{p_2}{p_1} = \frac{2\gamma M_1^2}{\gamma+1} - \frac{\gamma-1}{\gamma+1}, \text{ and} \quad (9)$$

$$\frac{T_2}{T_1} = \left(\frac{2\gamma M_1^2 - (\gamma - 1)}{(\gamma + 1)}\right)\left(\frac{2 + (\gamma - 1)M_1^2}{(\gamma + 1)M_1^2}\right) . \quad (10)$$

The c parameter provides a link to the flame equations. A high value of c implies high values of M_1 and of the pressure and temperature ratios at the shock, with a consequent increased propensity for autoignition.

3. Values of autoignition delay times of stoichiometric hydrogen/oxygen mixtures

In [1] it is estimated that the attainment of a DDT in a duct of 7 m length would require a value of τ_i of less than 3.8 ms. In the present study, the procedure adopted was to identify the values of *c* and the shock conditions necessary to generate values of τ_i of 0.05, 0.1, 1 and 5 ms. Bearing in mind the practical length of a detonation tube, autoignition delay times, τ_i, of the order of 1 ms might be necessary for the onset of autoignition and a DDT, without excessive tube lengths.

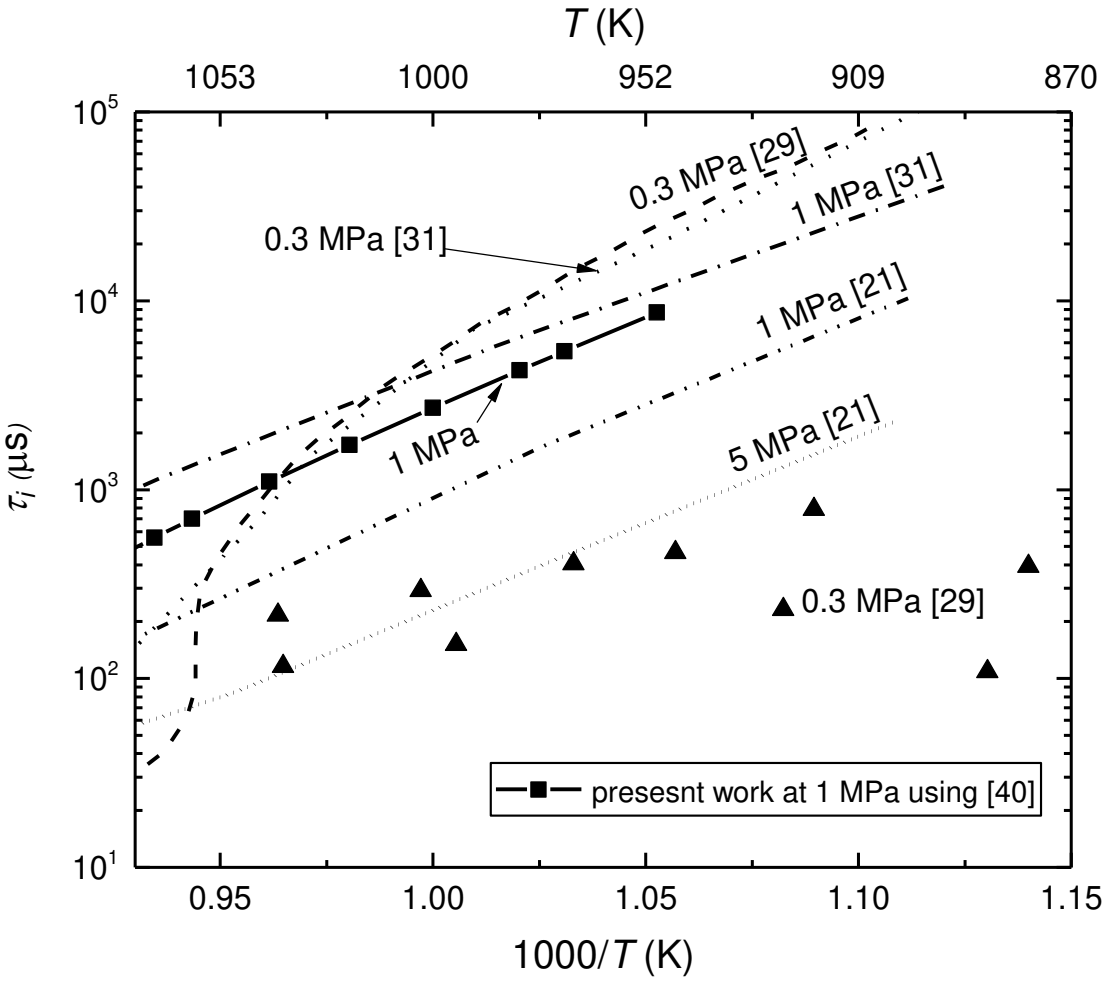

Fig. 2: Autoignition delay time of stoichiometric H_2/O_2 mixture at different temperatures and pressures > 0.1 MPa.

Many chemical kinetic modelling studies [17, 18, 20, 21, 29-31] have yielded τ_i values for stoichiometric H_2/O_2 at different pressures and temperatures. In an early study, Voevodsky and Soloukhin [29] measured τ_i in a shock tube at 0.1, 0.2 and 0.3 MPa, and compared these values with those from a chemical kinetic model. The comparison showed discrepancies at low temperatures. In a later experimental study on explosion limits with strong and weak autoignition, Meyer and Oppenheim [17] employed the kinetic schemes of Skinner and Ringrose [32] and Gardiner and Wakefield [33] to obtain τ_i at different temperatures, in the pressure range 0.02 to 0.2 MPa.

Ivanov et al. [20] studied the effect of the width of the no-slip wall duct at different diameters on the onset of detonation for stoichiometric H_2/O_2. The study was performed under atmospheric conditions with different chemical kinetics in six reaction schemes [34-39] and a one-step Arrhenius kinetic scheme.

Liberman et al. [21] employed a detailed chemical kinetics model to compute τ_i for stoichiometric H_2/O_2 and H_2/air between 0.001 to 5 MPa. Values of τ_i for stoichiometric H_2/O_2 at sub-atmospheric pressures were included in the mathematical model of Smirnov et al. [31] in the range 0.01 to 10 MPa.

These values of τ_i for stoichiometric H_2/O_2 from [21] and [31] at different temperatures, for pressures above atmospheric, are shown in Fig. 2. Also shown are the earlier computed and lower experimental (triangle symbol) data of Veovodsky and Soloukhin [29]. Of particular interest is the sharp decrease in τ_i at the highest temperatures when the pressure falls to 0.3 MPa.

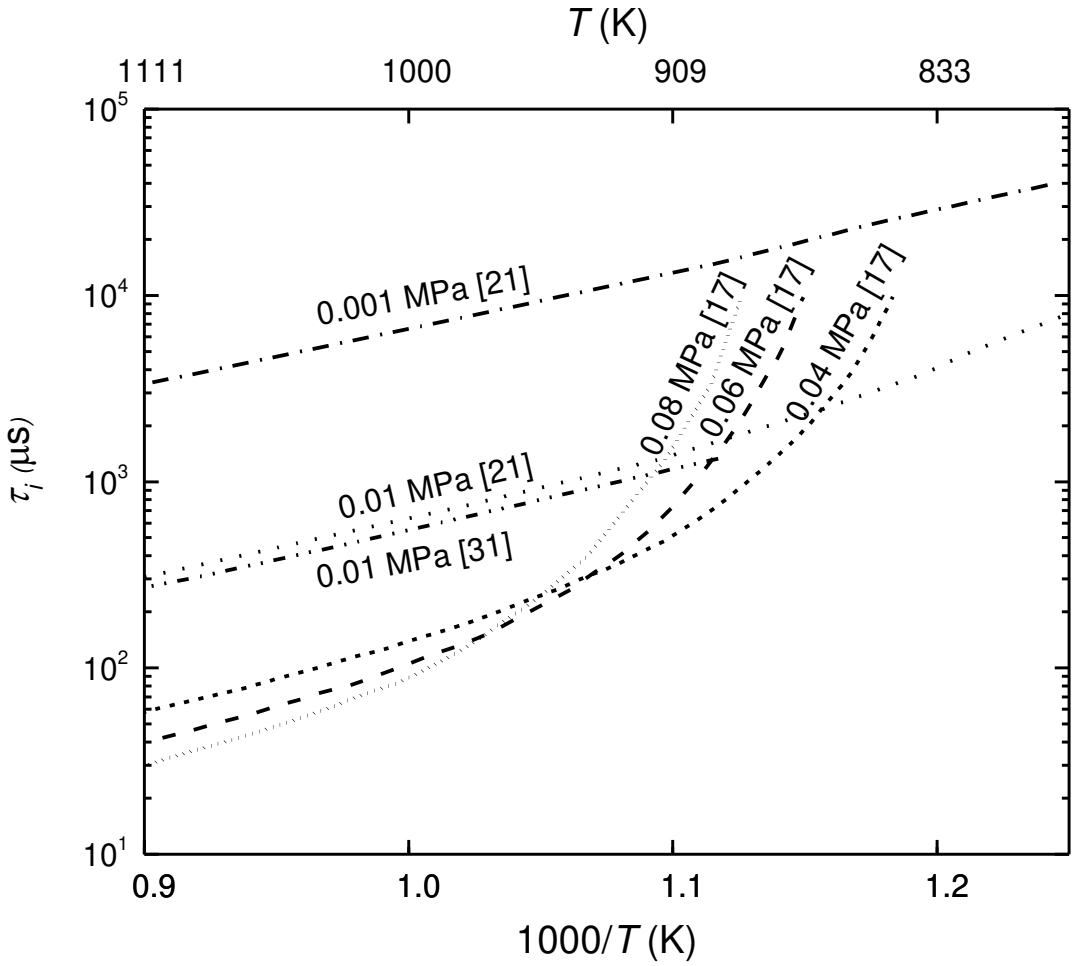

Fig. 3: Ignition delay time of stoichiometric H_2/O_2 mixture at different temperatures and sub-atmospheric pressures.

Figure 3 shows values of τ_i at sub-atmospheric pressures, and the same trend continues down to about 0.04 MPa, when it is reversed, and τ_i increases with pressure decrease.

The low pressure data in Fig. 4 compare earlier values of Meyer and Oppenheim [17] with the current computations using the Varga mechanisms [40] at pressures of 0.04, 0.06 and 0.08 MPa. Low pressures, combining low values of τ_i and high values of ν are conducive to laminar DDT.

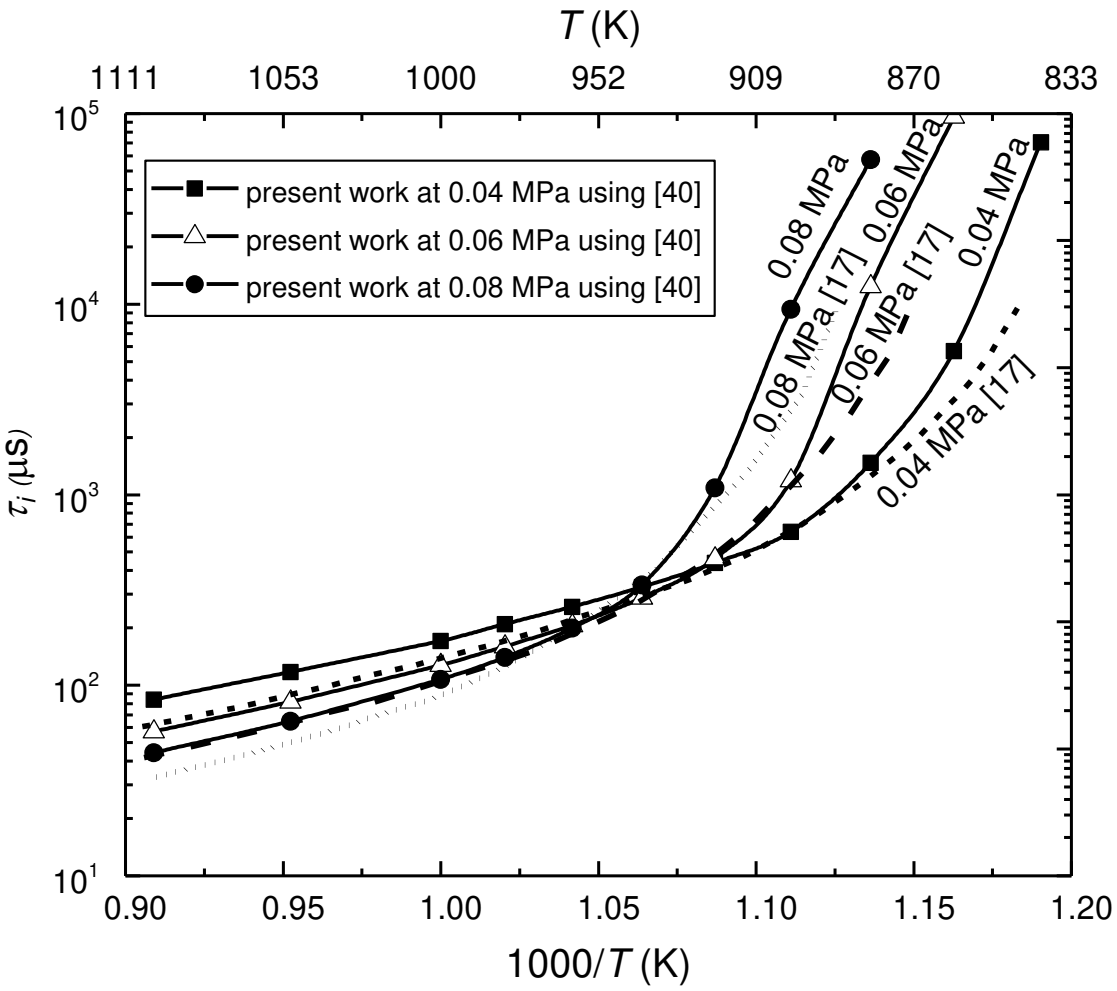

Fig. 4: Comparison of ignition delay time between Meyer and Oppenheim[17] study and present work using Varga mechanism [40].

Much of the available data on τ_i at 0.1 MPa are shown for different temperatures in Fig. 5. All of these values are computed, except the experimental results of Veovodsky and Soloukhin [29], which again are significantly less than the modelled values. The modelled results of Liberman et al. [21], and Smirnov et al. [31] are also shown. The present focus is on the range, $833 \leq T \leq 1111$ K. There continues to be uncertainties in the chemical kinetic details of what might appear to be a relatively simple, yet very important, oxidation. There is a maximum spread of about two orders of magnitude in values of τ_i.

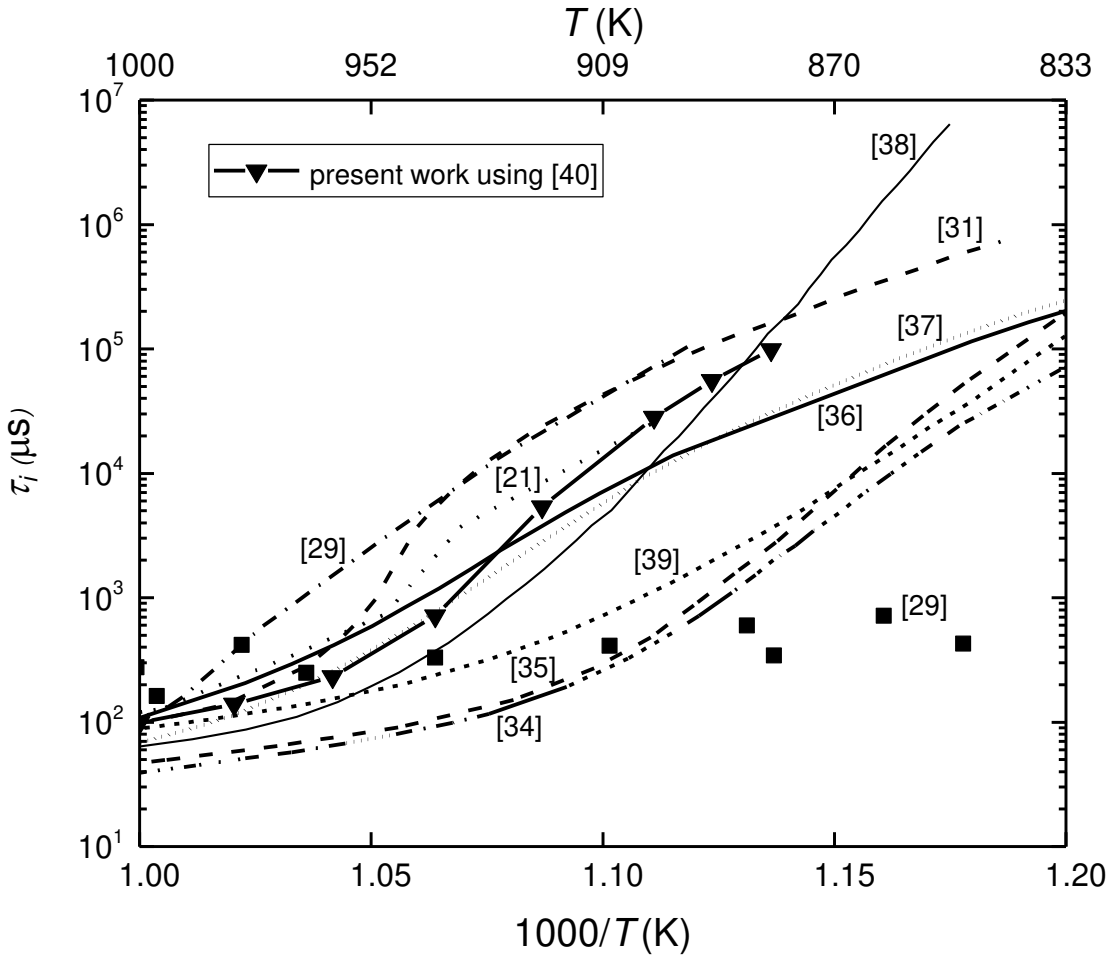

Fig. 5: Autoignition delay time of stoichiometric H_2/O_2 at different temperatures at 0.1 MPa.

Figure 6 shows values of τ_i, judged appropriate, and utilised in the present study. The lowest values of τ_i occur at the highest temperatures between 0.01 and 0.04 MPa. The review in [41] favours that of Kéromnès et al. [42], optimised by Varga et al.[40], and based on the CHEMKIN code [43]. This was employed in the present study, after review of the results shown in Figs. 2, 4, 5 and 6. These current computations give values close to the average of all the data in Fig. 5.

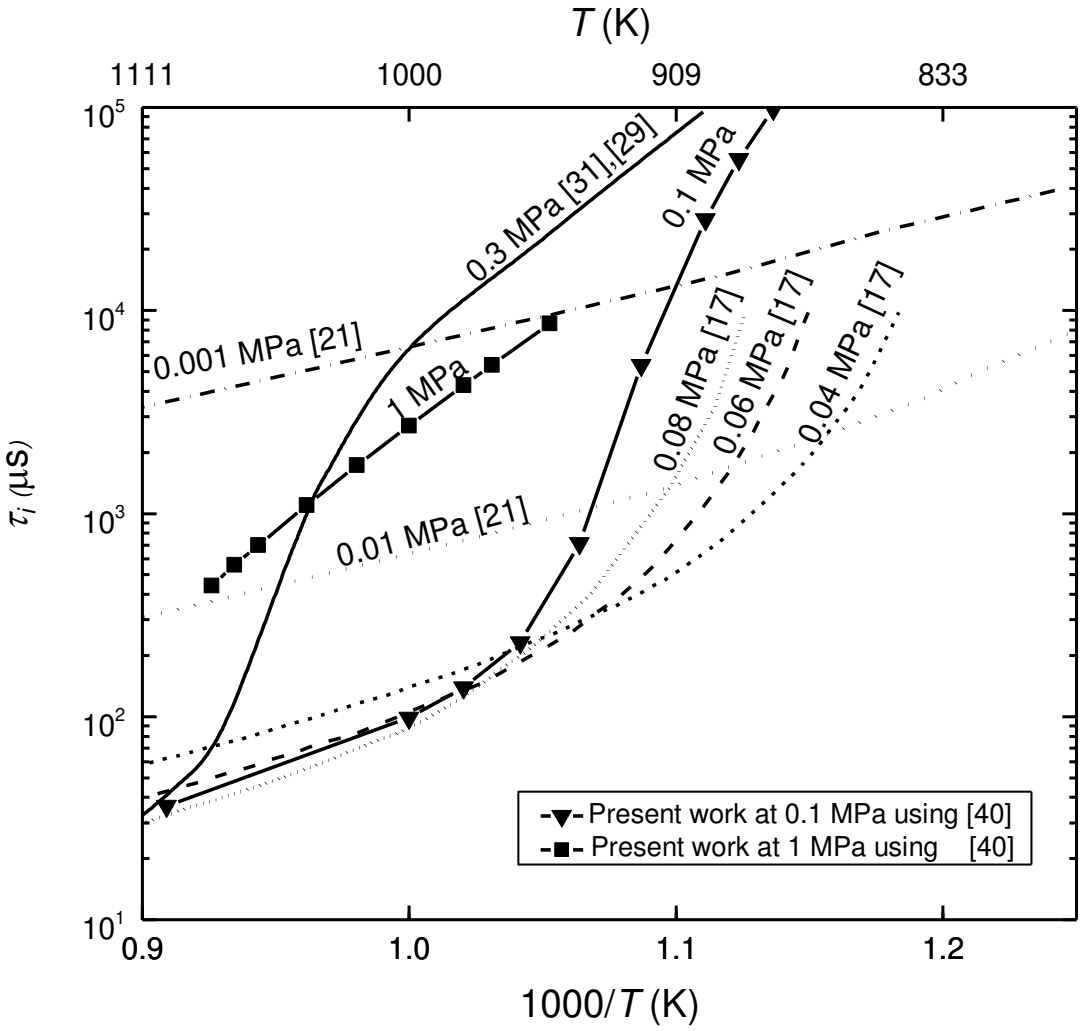

Fig. 6: Autoignition delay times of stoichiometric H_2/O_2 used in this current study.

Below 1000 K, values of τ_i peak between 0.1 and 0.3 MPa and then decrease with decreasing P down to about 0.06 MPa. They then increase with further decrease in pressure. From Fig. 6 a regime of minimal τ_i exists below 0.08 MPa and above 900 K, characterised by low τ_i and activation energies, given by:

$$E/R = \partial\, ln\tau_i/\partial(1/T). \tag{11}$$

The present analysis is for a variety of conditions, with the initial pre-shock temperature, T_1, equal to either 300 or 375 K. It is necessary to derive values of c for the different values of τ_i. For a given τ_i, associated values of T_2 and P_2 are identified in Fig. 6. For the given value of T_2, because T_1 is known, M_1 can be found from Eq. (10). This enables c to be found from Eq. (7). Values of c are consequently a function of T_2 only. In the same way, with the same value of M_1, because P_2 is known, the pre-shock pressure, P_1, can be found from Eq. (9). This approach enables isobars to be constructed based

on different values of P_2 and P_1, as shown in Fig. 7 for T_1 = 300 K. The isobars are labelled with the value of P_1. Values of c are shown for different values of T_2 to the right of the P_1 = 0.1 MPa isobar.

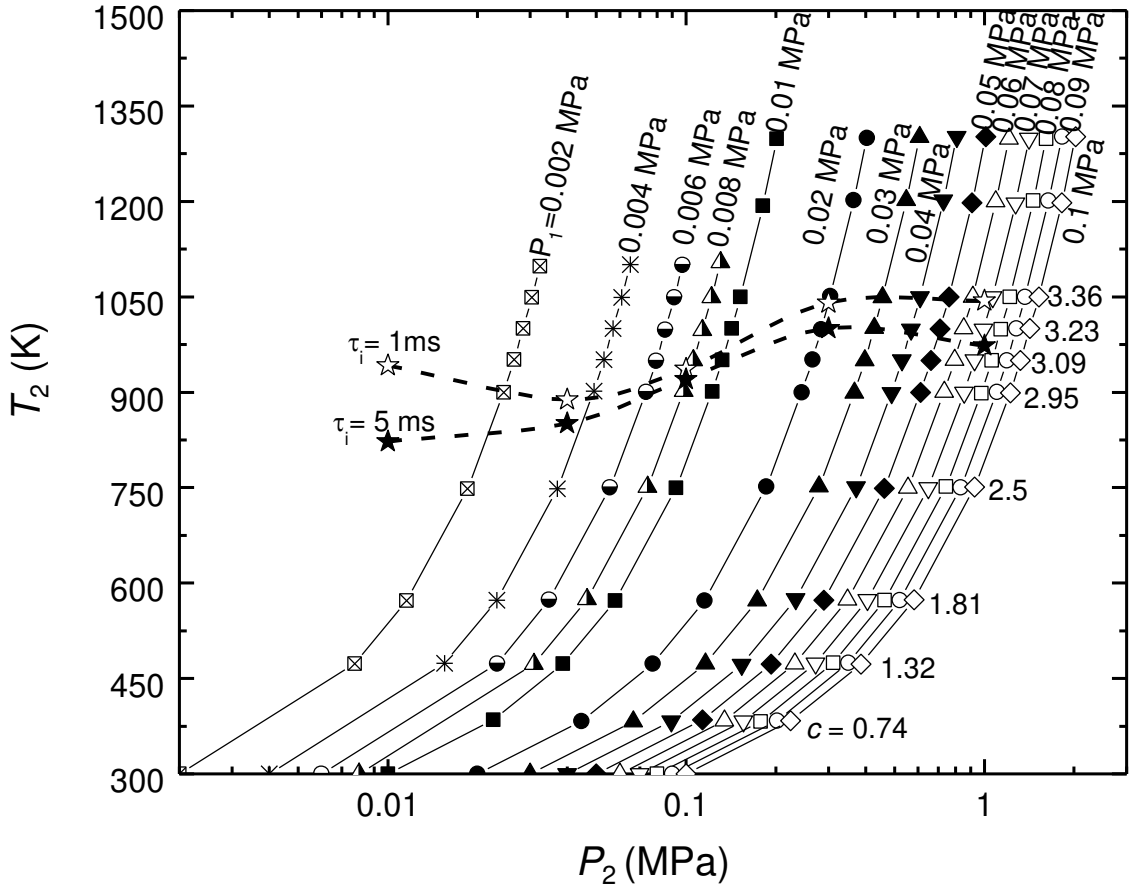

Fig. 7: Different isobars, showing the $T_2/P_2/c$ relationship for T_1 = 300 K, and τ_i values of 1 and 5 ms. Values of c on the right of P_1 = 0.1 MPa isobar.

4. Values of laminar burning velocities

After the shock, values of pressures and temperatures can be high, so that there is a dearth of values of u_ℓ, not least because of the increased hazard in making measurements. Bartholomé [44] measured u_ℓ for stoichiometric H_2/O_2 at 298 K and 0.1 MPa, using a burner. Koroll and Mulpuru [45] later made measurements under atmospheric conditions for the stoichiometric mixture with diluents using a nozzle-burner.

Gelfand et al. [46] reviewed the variations of u_ℓ with temperature for stoichiometric H_2/O_2 at atmospheric pressure, using burner results from Edse and Lawrence [47] and the computations of Kusharin et al. [48]. The experimental measurements were confined to maximum values of about 500 K. Computed values covered a wider range. Kuznetsov et al. [49] calculated u_ℓ for the mixture using the FP code [50] in the pressure range 0.02 to 0.8 MPa, at 300 K.

Numerical and experimental evaluations of u_ℓ for stoichiometric H_2/O_2 mixture in [51] have different proportions of steam between 0.1 and 7.2 MPa and temperatures from 383 to 573 K. Steam concentrations were between 0 and 80% H_2O. The highest u_ℓ values without steam were 29.8 and 24.9 m/s at 1 and 7.2 MPa, respectively, and 573 K. The burning velocity was calculated using four different H_2/O_2 kinetic mechanisms. Computed u_ℓ data, using the Boivin reduced mechanism [52], extending to 10 MPa and 750 K, have been presented by Mari et al. [53].

These data included in Fig. 8, show the effect of temperature, up to about 800 K, at atmospheric pressure, for stoichiometric H_2/O_2, along with data from six different studies. Values of u_ℓ at T and P are empirically correlated over a given range of T and P by:

$$u_l = u_{l0}\left(\frac{T}{T_0}\right)^{\alpha}\left(\frac{P}{P_0}\right)^{\beta}, \tag{12}$$

with α and β numerical constants, and T_0 and P_0 a reference temperature and pressure. In the present case these are 300 K and 0.1 MPa. Values of α and β were plotted against maxima of P or T over the respective ranges and these values were extrapolated to values at higher P and T. The associated extrapolated values of u_ℓ are shown by the broken curve, up to 1100 K.

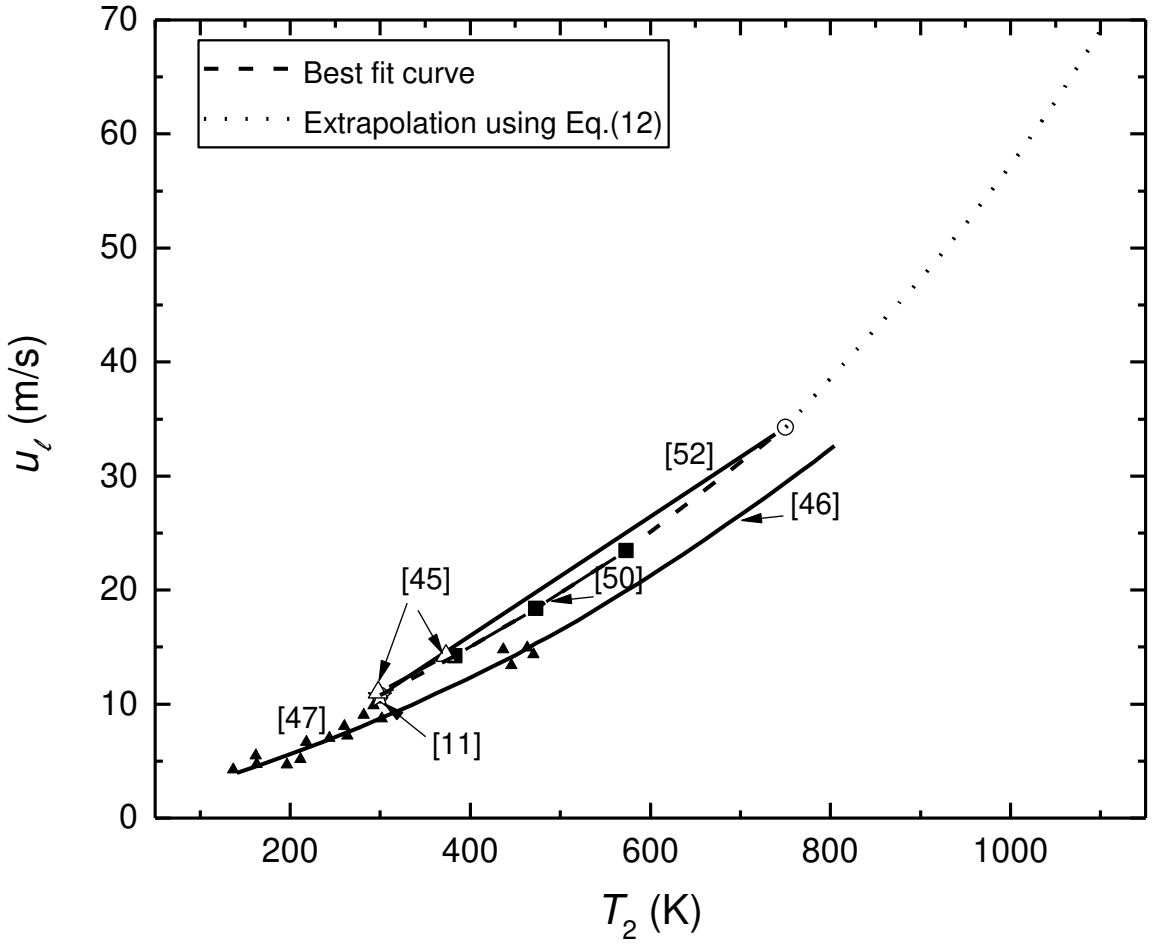

Fig. 8: Measured and computed values of u_l for stoichiometric H_2/O_2 at atmospheric pressure. The dotted curve is the extrapolation, to 1100 K using Eq. (12).

The effect of pressure is shown for different temperatures in Fig. 9. The computed data in [51] extended to 7.2 MPa and employed a variety of different reaction mechanisms. The Lutz mechanism [54] was recommended in [51], due to its good agreement with that of Maas and Warnatz [55]. Gelfand et al. [46] employed kinetic simulations for pressures up to 10 MPa at 298 K. The Boivin reduced mechanism [52] was used to calculate u_ℓ at 300 K between 0.1 and 10 MPa, and 750 K at 0.1 MPa [53]. These are plotted in Fig. 9 in the form of different isothermal values of u_ℓ as a function of the pressure P_2.

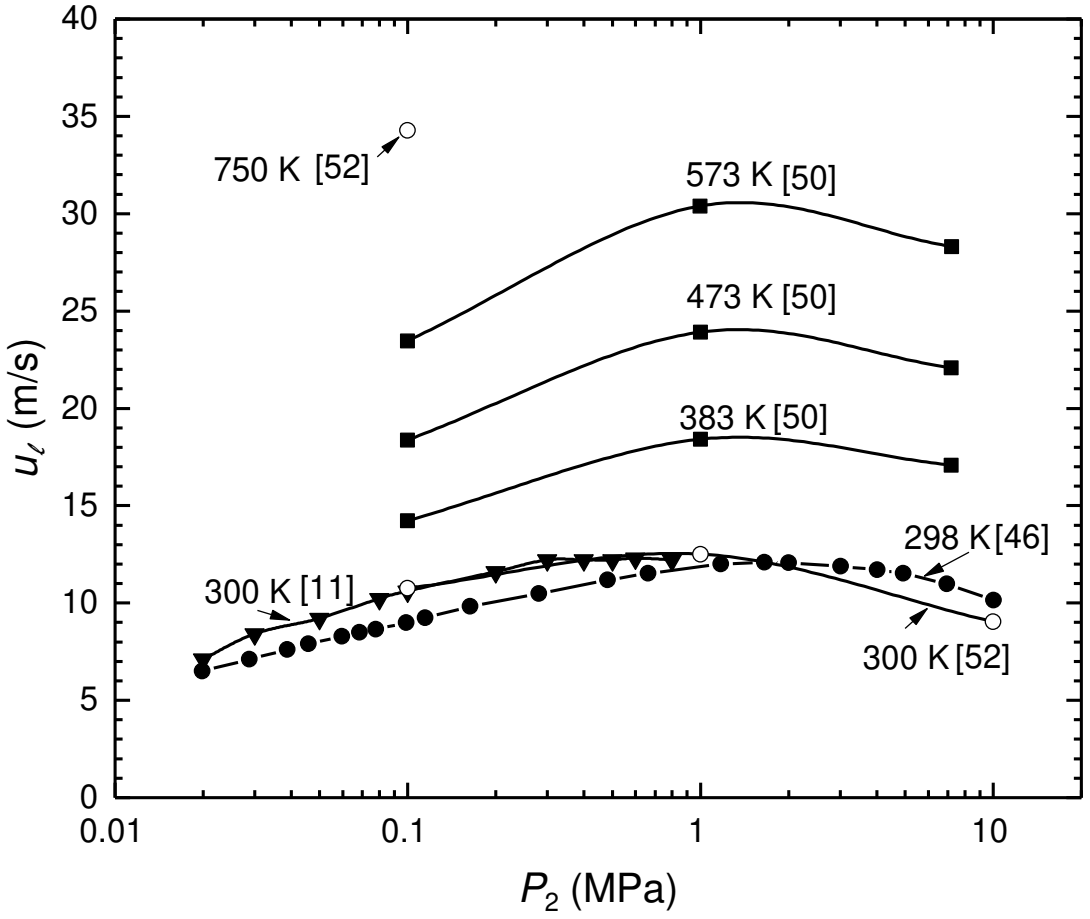

Fig. 9: Measured and computed values of u_ℓ for stoichiometric H_2/O_2 for different temperatures up to 750 K from different sources.

Figure 10 presents an extensive range of experimental, theoretical and extrapolated values of u_ℓ plotted against pressure for different isotherms relevant to the present study. Temperatures extend to 1100 K and pressures to 7.2 MPa. Extrapolated values are indicated by dotted curves. There is clearly a dearth of data at the higher temperatures, with excessive reliance on extrapolated values. An essential role of the u_ℓ data is, for a given value of c, the derivation of the minimal value of A/a for autoignition from Eq. (8). This value, along with that of σ, also enable S_f to be found from Eq. (1).

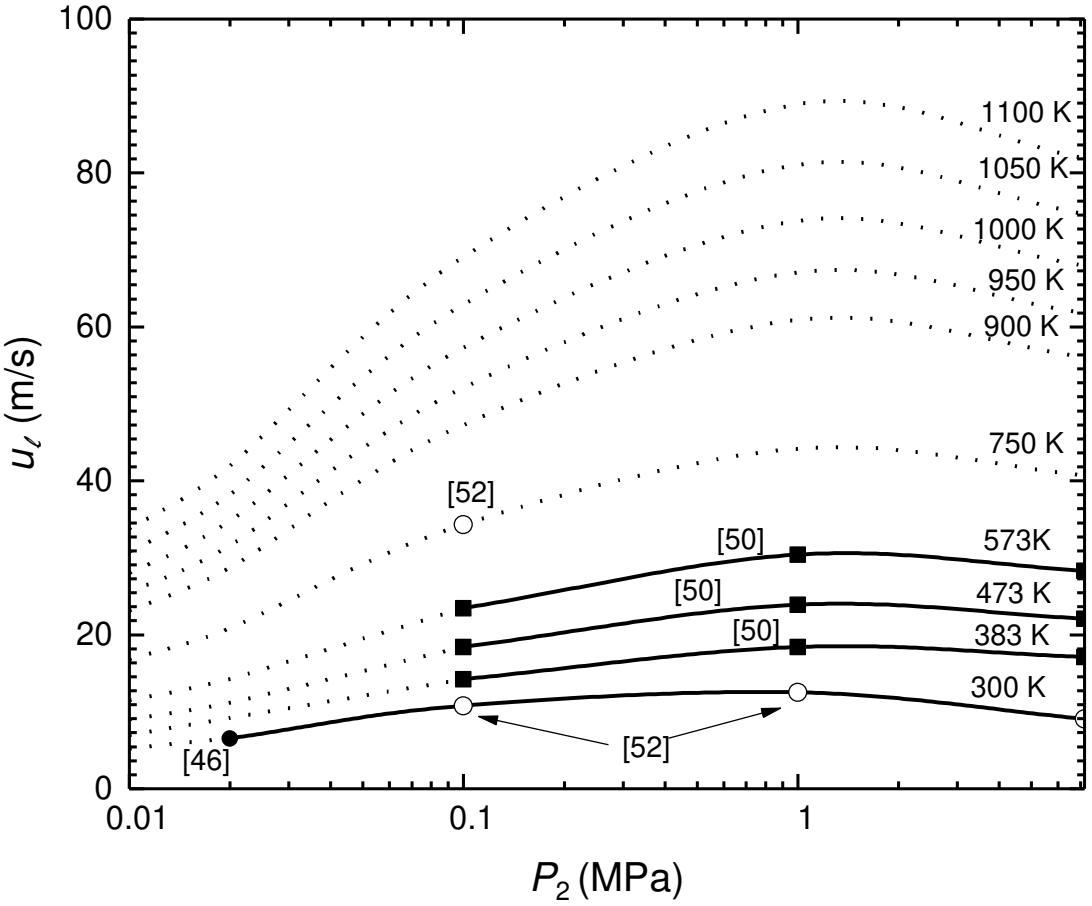

Fig. 10: Variations of u_ℓ for stoichiometric H_2/O_2 with pressure and temperature. Extrapolated values indicated by broken curves.

5. Laminar flame propagation in a tube of circular cross section

A high area ratio, A/a, is necessary for the attainment of a sufficiently high value of S_g, and consequently of c, for autoignition. For laminar flames the increase in flame area is entirely due to the increasing elongation of the flame front accompanying increases in u_ℓ, both of which increase S_g. Values of A/a are significantly larger than for turbulent flames.

The explosive growth in A/a results in a very rapid acceleration in S_g as autoignition is approached. The numerical simulations of Gamezo and Oran [26] of flame propagation of stoichiometric acetylene/oxygen in hypodermic tubes revealed rapidly accelerating flames that attained values of A/a of up to 30 in 0.5 ms in channel lengths of up to 8 cm. As the boundary layer developed, so did the velocity profile across the channel and the shape of the flame was similar to the velocity profile. With such a similarity the flame length is proportional to S_g.

In a study of the more sedate transition of a laminar flame from a spherical kernel to a finger-shaped front at the entry to a tube, Bychkov et al. [56] derived an approximate expression for A/a:

$$A/a = \frac{2\sigma^2}{\sigma + 1}. \tag{13}$$

As the flame thickness tended to zero, A/a tended to 14.

The attainment of a laminar DDT is enhanced by a high value of A/a. With a larger diameter, of 21 mm, Keramptam et al. [57], observed a rapid acceleration of a stoichiometric propane/air flame as it rapidly elongated, attaining an an A/a value of 9.3 after 12 ms in a duct length of 1.6 m.

With a parabolic distribution of the flow velocity, u, at radius, r, in a tube of diameter, D, is given by [58]:

$$u = 2S_g(1 - 4\,r^2/D^2). \tag{14}$$

The maximum velocity is $2S_g$ at the centre of the tube, and the flow strain rate is a maximum at the tube walls, given by:

$$(du/dr)_m = 8\,S_g/D\ . \tag{15}$$

Although the explosive increases in both u_ℓ and A/a very effectively increase S_g, the increasingly high strain rate at the tube walls due to S_g can lead to localised flame extinctions there and flame flashback.

To assess this possibility for laminar flames, a generalised laminar extinction Karlovitz stretch factor, K_{ql+} has been employed in an attempt to generalise the accumulated data on such extinctions. This is the hydrodynamic strain rate normalised by a chemical time, given by the laminar flame thickness, expressed by ν/u_ℓ , divided by u_ℓ [59], Hence,

$$K_{ql+} = (8\,S_g/D)\,\nu/{u_\ell}^2\ . \tag{16}$$

For strain rate Markstein numbers between -2 and +2, K_{ql+} is approximately unity. Because of the difficulty of generating and measuring extinguishing stoichiometric H_2/O_2 flames, no data are known to the authors for stoichiometric H_2/O_2 extinction, but some data are available for lean H_2/air flames [60]. An extensive extrapolation of these data to the stoichiometric H_2/O_2 conditions suggested a value of K_{ql+} of about 2. While a degree of quenching might be tolerated, an increase in D would be necessary to reduce it. Close to this limit, it was calculated that the viscous dissipation term in the

energy equation showed the mixture could be sufficiently heated to autoignite, although heat loss to the wall would reduce this. For some time there has been strong evidence for such boundary layer-induced autoignitions [24]. The numerical simulations for H_2/O_2 mixtures of Dziemińska and Hayashi [61] show the shock wave heating the boundary layer. This is followed by secondary shock waves, between the main shock and the flame, further heating the boundary layer, to the point of autoignition, with transition to detonation.

With micro tubes the heat loss will be significant, although insufficient to inhibit strong flame acceleration and possible transition to detonation. In the earlier stages, the effect would be to require a longer transitional distance. In the final stage of a transition to autoignition, there is a similar effect. It is estimated for Condition B, in Table 2(b) below, with D_c = 0.494 mm, that in the critical region between the shock wave and the flame, heat transfer would reduce the mixture temperature by about 36 K from 997 K. In practice, this would require further flame acceleration and compression before autoignition. If the large value of K_{ql+} proved to be not so inhibiting, the condition labelled E in Table 2(a) below, would have a reduced heat transfer rate due to the larger D_c of 1.35 mm. In this case, the mixture temperature 1131 K would only fall by 8 K.

6. Results

The crucial limiting conditions for autoignition in laminar flow rest upon the attainment of the limiting Reynolds number, Re_c = 2300 for such flow. The corresponding critical values of D are D_c. These are listed in Tables 1 (a) and 1 (b) for T_1 = 300 K, with τ_i =1 and 5 ms, and in Tables 2 (a) and (b) for the more reactive conditions of T_1 = 375 K with τ_i = 0.1 and 0.05 ms. All Tables cover the same three different values of P_2, whilst Tables 1(a) and (b) additionally cover two further values. Tables 1 tend to be characterised by higher values of c and lower values of T_2, and Tables 2 by lower values of c and higher values of T_2. The parameters are presented, reading from left to right, in the order they are presented at the ends of Sections 3 and 4. Values of D_c are found from the values of S_g and ν. In addition to Re_c, K_{ql+} can be a limiting factor, and these values comprise the final listing in the Tables. Values of σ, γ and ν were found from the GasEq code [621] and those of S_g were found from the different values of c and Eq. (8).

Bearing in mind the restrictive influences of high values of K_{ql+} and the practical problems of values of D_c less than 0.4 mm, only four conditions seem practical for autoignition in laminar flow. These conditions are identified by A, B, C, D, adjacent to the final K_{ql+} column.

Table 1(a): Autoignitions of stoichiometric H_2/O_2 with $\tau_i =$ 1 ms at T_1 = 300 K.

T_1 (K)	P_2 (MPa)	T_2 (K)	c	M_1	P_1 (MPa)	S_g (m/s)	u_ℓ (m/s)	A/a	σ	ν (m^2/s)	S_f (m/s)	D_c (mm)	K_{ql+}	
300	0.01	941.9	3.07	3.37	0.00076	1381	22.3	38	2.62	2.6E-3	2231	4.3	13.3	
300	0.04	888	2.9	3.23	0.0033	1313	36.5	19	2.9	5.8E-4	2007	1	4.4	
300	0.1	936	3.06	3.36	0.0077	1374	50.7	14.7	2.83	2.6E-4	2123	0.43	2.6	**C**
300	0.3	1040	3.33	3.61	0.02	1498	73	12.3	2.67	1.0E-4	2394	0.16	1.5	
300	1	1043.8	3.34	3.62	0.066	1502	80	10.7	2.76	3.0E-5	2355	0.05	1.2	

Table 1(b): Autoignitions of stoichiometric H_2/O_2 with $\tau_i =$ 5 ms at T_1 = 300 K.

T_1 (K)	P_2 (MPa)	T_2 (K)	c	M_1	P_1 (MPa)	S_g (m/s)	u_ℓ (m/s)	A/a	σ	ν (m^2/s)	S_f (m/s)	D_c (mm)	K_{ql+}	
300	0.01	822	2.72	3.05	0.00094	1224	17.6	35.3	2.96	2.1E-3	1848	3.87	16.7	
300	0.04	851	2.81	3.13	0.0036	1264	35	18	3	5.5E-4	1895	0.997	4.5	
300	0.1	920	3.01	3.31	0.008	1354	49	14.6	2.9	2.5E-4	2074	0.42	2.6	**D**
300	0.3	1000	3.23	3.5	0.021	1451	67	12.3	2.77	9.5E-5	2273	0.15	1.6	
300	1	973	3.16	3.45	0.073	1419	70	10.4	2.94	2.7E-5	2150	0.044	1.4	

Table 2(a): Autoignitions of stoichiometric H_2/O_2 with $\tau_i =$ 0.05 ms at T_1 = 375 K.

T_1 (K)	P_2 (MPa)	T_2 (K)	c	M_1	P_1 (MPa)	S_g (m/s)	u_ℓ (m/s)	A/a	σ	ν (m^2/s)	S_f (m/s)	D_c (mm)	K_{ql+}	
375	0.04	1131	2.97	3.27	0.0032	1488	57.7	19.5	2.323	8.8E-4	2614	1.35	2.3	**E**
375	0.1	1061	2.81	3.13	0.0089	1407	64.23	14.3	2.532	3.2E-4	2325	0.517	1.7	**A**
375	0.3	1092	2.88	3.19	0.026	1443	78.6	11.8	2.556	1.1E-4	2371	0.175	1.2	

Table 2(b): Autoignitions of stoichiometric H_2/O_2 with $\tau_i =$ 0.1 ms at T_1 = 375 K.

T_1 (K)	P_2 (MPa)	T_2 (K)	c	M_1	P_1 (MPa)	S_g (m/s)	u_ℓ (m/s)	A/a	σ	ν (m^2/s)	S_f (m/s)	D_c (mm)	K_{ql+}	
375	0.04	1031.7	2.73	3.06	0.00372	1371	48	18.8	2.52	7.5E-4	2272	1.26	2.8	
375	0.1	997	2.65	2.98	0.0098	1327	56.9	13.9	2.678	2.8E-4	2118	0.494	1.9	**B**
375	0.3	1072.6	2.83	3.15	0.0263	1420	75.8	11.73	2.597	1.1E-4	2309	0.173	1.2	

7. Discussion

A key factor is that S_g must be large enough to create autoignition and, yet not so large as to exceed Re_c. As a consequence, ν should be large in order to make D as large as possible. This also beneficially reduces K_{ql+}. From Table 1(a), for T_1 = 300 K and τ_i = 1 ms, if the value of K_{ql+} = 4.5, which exceeds the extrapolated limit of 2, were to be accepted then D could be 1 mm. The corresponding value of A/a of 18 is rather high but might be attainable. More cautiously, a lower value of D = 0.43 mm would probably be more practical, with K_{ql+}= 2.6 and A/a = 14.7. In practice, if Re_c were to be exceeded, micro-turbulence would develop on the large flame area, A, increasing the burning velocity and further strengthening the shock. Flame imaging of such flames suggests their appearance would initially be indistinguishable from that of a laminar flame.

It is difficult to know the upper limit to K_{ql+}, because of the uncertainty in the extrapolated value and the degree of quenching that might be tolerated, yet partially countered by dissipation-induced autoignition, With an upper limit of 2.6, only the bottom three entries in Tables 1(a) and 1(b) would support a purely laminar autoignition. Tables 2 (a) and (b) cover more reactive mixtures, resulting from preheating to 375 K. For τ_i = 0.05 ms, a maximum value of D_c of about 1.3 mm is possible, albeit at a low value of P_1 and high value of A/a. At the higher values of P_2 of 0.3 MPa, higher values of S_g are required, and D becomes impractically smaller.

The laminar flames become more elongated with increasing u_ℓ, leading also to an associated increase in A/a. Consequently, autoignition is enhanced, not only by a high value of u_ℓ, but also by the associated increase in flame surface area. Of the different values of D_c listed in the Tables, only those four between 0.42 and 0.52 mm would seem to be in any way practical. With τ_i = 1 ms, autoignition is probable and practical. At the higher values of S_g, D_c becomes impractically small, with values of less than 0.1 mm.

Having established the four most probable conditions, A - D, in Tables 1 and 2, for autoignitions, the likelihood of a detonation remains to be assessed. In addition to a developing detonation, the other possibilities, following upon autoignition, include continuing normal flame propagation, and thermal explosion. These regimes were located relative to the detonation peninsula, shown in Fig. 11. This plots the ratio of acoustic to autoignitive velocity, ξ, against ε. The latter is the ratio of the residence time within the hot spot of the pressure pulse that is generated by the rate of change of the heat release rate, to the duration for the heat release, the excitation, time, τ_e [63, 64].

The auto- ignitive velocity, is given by:

$$u_a = (dr/dT)(dT/d\tau_i) = (dr/dt)(\tau_i E/RT^2)^{-1}. \quad (17)$$

A critical value of the temperature gradient, $(dT/dr)_c$ is attained when u_a is equal to the acoustic velocity, a, and:

$$a = (dr/dT)_c(\tau_i E/RT^2)^{-1}\text{ , with} \quad (18)$$

$$\xi = a/u_a = (dr/dT)/\,(dr/dT)_c. \quad (19)$$

If the radius of the hot spot is r, with the excitation time τ_e, then

$$\varepsilon = (r/a\tau_e). \quad (20)$$

Values of τ_i and E/R at P_2 and T_2, for the four conditions A to D, were obtained from Fig. 6. Those of τ_e were found by computing the temporal heat release rates, as outlined in [65], using the Cantera code [66].

The pressure, P_2, for the four selected diameters was the same and equal to 0.1 MPa, but the temperatures, T_2, were variable. The values of these parameters, and others from which they are derived, are given in Table 3. A value of $(dT/dr)_c$ = 1 K/mm, occurred at T_2 = 1040 K. To evaluate ξ it is necessary to attribute a general value to (dT/dr) in Eq. (19). This value is determined less by the physico-chemical parameters and more by micro-flow patterns and energy transfers that are variable, and are stochastic. A value of -2 K/mm was chosen, on the basis of engine and other measurements [64].

Table 3. Autoignition parameters for atmospheric stoichiometric H_2/O_2 mixture at dT/dr = -2 mm

	T_1 (K)	T_2 (K)	τ_i (ms)	τ_e (μs)	$\frac{\tau_i}{\tau_e}$	$\frac{E}{R}$ (K)	$\frac{E}{RT}$	$\bar{E}$	a (m/s)	$\frac{E}{RT^2}$ (K^{-1})	$(\frac{d\tau_i}{dT})^{-1}$	$\left(\frac{dT}{dr}\right)_c$ (K/mm)	u_a (m/s)	ξ	ε	$\frac{dlnT}{d\bar{r}}$	$\frac{\bar{E}\ dlnT}{d\bar{r}}$
A	375	1061	0.05	2	25	9,519	8.97	225.2	995.8	0.0085	2,355,785	2.37	1177.9	0.85	2.51	0.0094	2.11
B	375	997	0.1	1.98	52	17,149	17.2	895	966.8	0.0173	562,733	0.58	281.37	3.44	2.61	0.00998	8.93
C	300	936	1	1.93	504	44,141	47.16	23,760	938.1	0.0504	20,413	0.012	10.21	91.9	2.76	0.0106	252.5
D	300	920	5	1.8	2778	59,161	64.28	178,568	930.5	0.0698	2863	0.003	1.432	650	2.99	0.0108	1930

The four chosen conditions studied are labelled A, B, C, D in the three Tables, are in the order of their decreasing T_2 values. Their coordinates in the ξ/ε diagram are shown in Fig. 11. Each point lies in a different one of the four, contrasting regimes. Of these, A and B, with T_1 = 375 K lie in the most reactive regimes, culminating in a thermal explosion and a developing detonation. In regime C, T_1 = 300 K combustion would be by autoignitive propagation, whilst in D, T_1 = 300 K, there would probably be normal flame deflagration. The flame would continue to accelerate into a turbulent regime, aided by the large A/a ratio created in the laminar flow, and probably would eventually autoignite.

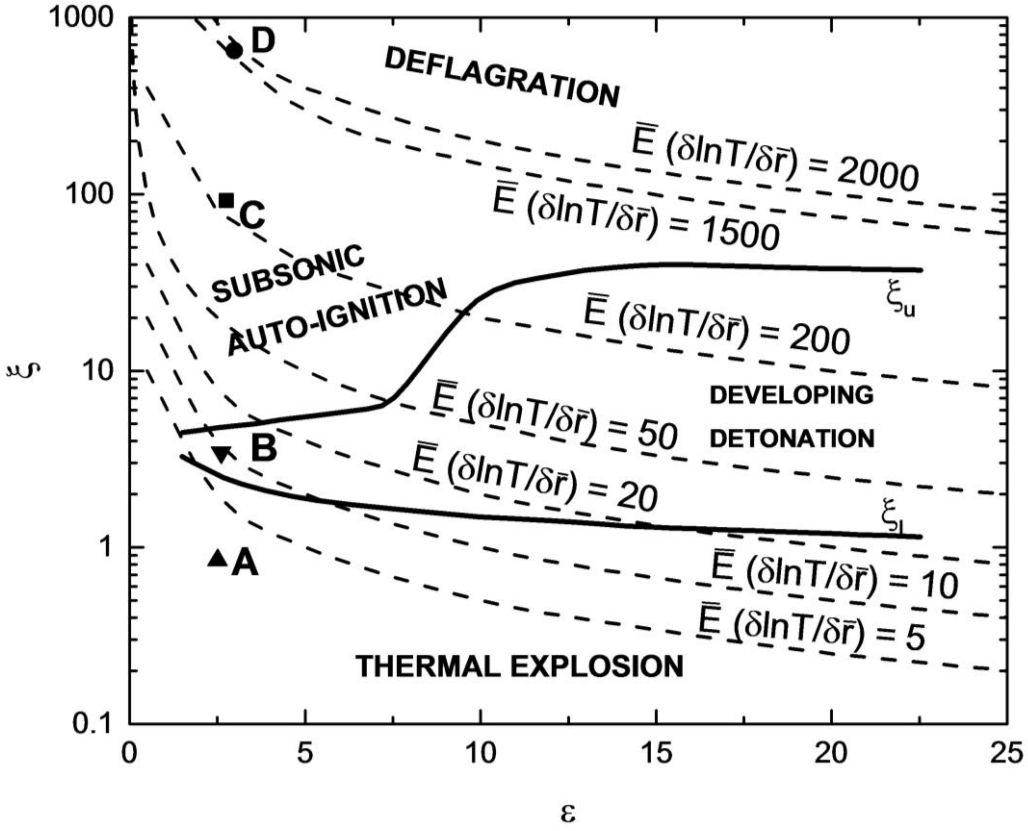

Fig. 11: Detonation peninsula diagram showing ξ/ε variations, and regime points A, B, C and D in order of decreasing temperature.

In a detonation, reaction might decouple from the shock and it has been found that the coherence and stability of a detonation are enhanced by low values of $(\tau_i/\tau_e)(E/RT) = \bar{E}$ [67-69]. To this product can be added $lnT/d\bar{r}$ [2], the dimensionless gradient at a hot spot, and it follows that:

$$\xi\varepsilon = \bar{E}(dlnT/d\bar{r}). \qquad (20)$$

Values of this product are given in Table 3, for an assumed hot spot radii of 5 mm. In Fig. 11 low values of the product are indicative of stable developing detonations. At the high values, autoignitive propagation begins to fail and be replaced by normal flame deflagrations.

As a further check on the propensity to undergo a laminar DDT, the marginal conditions for D_c= 1.35 mm in Table 2(a), with rather high values of A/a and K_{ql+}, were examined. If autoignition were to occur in this otherwise reactive mixture, either a thermal explosion or a detonation would develop. This would suggest the possibility of a laminar DDT, in hypodermic tubes of between 0.5 and 1.3 mm diameter, with T_1 = 375 K.

8. Conclusions

(i). There are uncertainties in the values of τ_i and τ_e that are relevant to the probability of laminar flow autoignition of stoichiometric H_2/O_2, despite using the most favourable hydrogen mechanism for values.

(ii). There are greater uncertainties in the necessarily extrapolated values of u_ℓ in Fig. 10.

(iii). Nevertheless, a laminar DDT appears to be probable in a rather narrow range of conditions with tube diameters close to 0.5 mm, at relatively low pressures, with T_1= 375 K.

(iv). Even without detonation, very high gas velocities can be generated using hypodermic tubes. There is significant heat loss from such tubes, but the main effect is to increase the tube length before transition.

(v). A characteristic of the growing pressurisation of the laminar flame is the large increases in both u_ℓ and A/a. The latter are significantly greater than those which occur in turbulent flames.

(vi). When the gas flow ahead of the H_2/O_2 accelerating flame causes Re to exceed Re_c, the flame image continues to be elongated and appears laminar for some time. This may explain why transitions have been described as laminar.

(vii). With the present data, only when T_1 is raised to 375 K do purely laminar developing detonations become possible for hypodermic tube diameters between about 0.5 and 1.35 mm.

Acknowledgements

The authors are grateful to the Egyptian Cultural and Educational Bureau and Port Said University for the financial support given to M.S. Inna Gorbatenko is also thanked for her help with the computations of τ_e.

References

[1] Bradley D, Lawes M, Liu K. Turbulent flame speeds in ducts and the deflagration/detonation transition, Combust. Flame 154 (1) (2008) 96-108.

[2] Bradley D. Autoignitions and detonations in engines and ducts, Phil. Trans. R. Soc. A 370 (1960) (2012) 689-714.

[3] Schmidt E H, Steinicke H, Neubert U. Flame and schlieren photographs of combustion waves in tubes, Symp. (Int.) Combust. 4 (1) (1953) 658-66.

[4] Dorofeev S, Sidorov V, Dvoinishnikov A, Breitung W. Deflagration to detonation transition in large confined volume of lean hydrogen-air mixtures, Combust. Flame 104 (1-2) (1996) 95-110.

[5] Lee J, Knystautas R, Chan C. Turbulent flame propagation in obstacle-filled tubes, Symp. (Int.) Combust. 20 (1) (1985) 1663-72.

[6] Obara T, Yajima S, Yoshihashi T, Ohyagi S. A high-speed photographic study of the transition from deflagration to detonation wave, Shock Waves 6 (4) (1996) 205-10.

[7] Chapman W R, Wheeler R V. The propagation of flame in mixtures of methane and air. Part IV. The effect of restrictions in the path of the flame, J. Chem. Soc. 129 (1926) 2139-47.

[8] Shchelkin K. Influence of tube roughness on the formation and detonation propagation in gas, J. Exp. Theor. Phys. 10 (1940) 823-29.

[9] Shchelkin K. Occurance of detonation in gases in rough-walled tubes, Sov. J. Tech. Phys. 17 (5) (1947) 613.

[10] Urtiew P, Oppenheim A. Experimental observations of the transition to detonation in an explosive gas, Proc. R. Soc. A 295 (1440) (1966) 13-28.

[11] Kuznetsov M, Alekseev V, Matsukov I, Dorofeev S. DDT in a smooth tube filled with a hydrogen–oxygen mixture, Shock Waves 14 (3) (2005) 205-15.

[12] Kuznetsov M, Liberman M, Matsukov I. Experimental study of the preheat zone formation and deflagration to detonation transition, Combust. Sci. Technol. 182 (11-12) (2010) 1628-44.

[13] Liberman M, Ivanov M, Kiverin A, Kuznetsov M, Chukalovsky A, Rakhimova T. Deflagration-to-detonation transition in highly reactive combustible mixtures, Acta Astronaut. 67 (7) (2010) 688-701.

[14] Liberman M, Ivanov M, Kiverin A, Kuznetsov M, Rakhimova T, Chukalovskii A. On the mechanism of the deflagration-to-detonation transition in a hydrogen-oxygen mixture, J. Exp. Theor. Phys. 111 (4) (2010) 684-98.

[15] Nagai K, Okabe T, Kim K, Yoshihashi T, Obara T, Ohyagi S. A study on DDT processes in a narrow channel, Shock Waves (2009) 203-08.

[16] Wu M H, Burke M P, Son S F, Yetter R A. Flame acceleration and the transition to detonation of stoichiometric ethylene/oxygen in microscale tubes, Proc. Combust. Inst. 31 (2) (2007) 2429-36.

[17] Meyer J, Oppenheim A. On the shock-induced ignition of explosive gases, Symp. (Int.) Combust. 13 (1) (1971) 1153-64.

[18] Ivanov M, Kiverin A, Liberman M. Hydrogen-oxygen flame acceleration and transition to detonation in channels with no-slip walls for a detailed chemical reaction model, Phys. Rev. E 83 (5) (2011) 1-16.

[19] Ivanov M, Kiverin A, Yakovenko I, Liberman M A. Hydrogen-oxygen flame acceleration and deflagration-to-detonation transition in three-dimensional rectangular channels with no-slip walls, Int. J. Hydrogen Energy 38 (36) (2013) 16427-40.

[20] Ivanov M, Kiverin A, Liberman M A. Flame acceleration and DDT of hydrogen-oxygen gaseous mixtures in channels with no-slip walls, Int. J. Hydrogen Energy 36 (13) (2011) 7714-27.

[21] Liberman M A, Kiverin A, Ivanov M. Regimes of chemical reaction waves initiated by nonuniform initial conditions for detailed chemical reaction models, Phys. Rev. E 85 (5) (2012) 1-16.

[22] Han W, Gao Y, Law C K. Flame acceleration and deflagration-to-detonation transition in micro-and macro-channels: An integrated mechanistic study, Combust. Flame 176 (2017) 285-98.

[23] Fukuda M, Dziemińska E, Hayashi A K, Yamada E, Tsuboi N. Effect of wall conditions on DDT in hydrogen-oxygen mixtures, Shock Waves 23 (2013) 191-200.

[24] Sivashinsky G I. Some developments in premixed combustion modeling, Proc. Combust. Inst. 29 (2) (2002) 1737-61.

[25] Kessler D, Gamezo V, Oran E. Simulations of flame acceleration and deflagration-to-detonation transitions in methane-air systems, Combust. Flame 157 (11) (2010) 2063-77.

[26] Gamezo V N, Oran E S. Flame acceleration in narrow channels: applications for micropropulsion in low-gravity environments, AIAA J. 44 (2) (2006) 329.

[27] Kuznetsov M, Ciccarelli G, Dorofeev S, Alekseev V, Yankin Y, Kim T. DDT in methane-air mixtures, Shock Waves 12 (3) (2002) 215-20.

[28] Zipf R K, Gamezo V, Sapko M, Marchewka W, Mohamed K, Oran E, Kessler D, Weiss E, Addis J, Karnack F. Methane-air detonation experiments at NIOSH Lake Lynn Laboratory, J. Loss Prevent. Process Ind. 26 (2) (2013) 295-301.

[29] Voevodsky V, Soloukhin R. On the mechanism and explosion limits of hydrogen-oxygen chain self-ignition in shock waves, Symp. (Int.) Combust. 10 (1) (1965) 279-83.

[30] Kiverin A D, Kassoy D R, Ivanov M F, Liberman M A. Mechanisms of ignition by transient energy deposition: Regimes of combustion wave propagation, Phys. Rev. E 87 (3) (2013) 1-10.

[31] Smirnov N N, Nikitin V F, Phylippov Y G. Hydrogen engines numerical modeling, Proceedings of XLI International Summer School-Conference APM, Russia, St. Petersburg (2013).

[32] Skinner G B, Ringrose G H. Ignition Delays of a Hydrogen-Oxygen-Argon Mixture at Relatively Low Temperatures, The Journal of Chemical Physics 42 (6) (1965) 2190-2.

[33] Gardiner W, Wakefield C. Influence of gasdynamic processes on the chemical kinetics of the hydrogen-oxygen explosion at temperatures near 1000 K and pressures of several atmospheres(Gas dynamic processes effects on hydrogen-oxygen explosion chemical kinetics, calculating ignition delays under steady conditions behind plane reflected shock waves), Astronautica Acta 15 (1969) 399-409.

[34] Starik A, Titova N. Kinetics of detonation initiation in the supersonic flow of the H_2+ O_2 (air) mixture in O_2 molecule excitation by resonance laser radiation, Kinetics and Catalysis 44 (1) (2003) 28-39.

[35] Bokhon Y A, Gal'burt V, Gostintsev Y. Explosion initiation in a gaseous mixture behind shock wave, Report No. 2-416, Institute of High Temperature Physics RAN, Moscow, 1998.

[36] Gal'burt V, Ivanov M, Petukhov V. Mathematical modeling of different combustion regimes, Chem Phys 26 (2007) 46-59.

[37] Popov N A. The effect of nonequilibrium excitation on the ignition of hydrogen-oxygen mixtures, Teplofizika vysokikh temperatur 45 (2) (2007) 296-315.

[38] Shatalov O, Ibraguimova L, Pavlov V, Smekhov G, Tunik Y V. Analysis of the kinetic data described oxygen-hydrogen mixtures combustion, 4th European Combustion Meeting (2009) paper 222.

[39] Smith G P, Golden D M, Frenklach M, Moriarty N W, Eiteneer B, Goldenberg M, Bowman C T, Hanson R K, Song S, Gardiner Jr W. GRI-Mech 3.0. Available: http://www.me.berkeley.edu/gri_mech (1999).

[40] Varga T, Nagy T, Olm C, Zsély I G, Pálvölgyi R, Valkó É, Vincze G, Cserháti M, Curran H, Turányi T. Optimization of a hydrogen combustion mechanism using both direct and indirect measurements, Proc. Combust. Inst. 35 (1) (2015) 589-96.

[41] Olm C, Zsély I G, Pálvölgyi R, Varga T, Nagy T, Curran H J, Turányi T. Comparison of the performance of several recent hydrogen combustion mechanisms, Combust. Flame 161 (9) (2014) 2219-34.

[42] Kéromnès A, Metcalfe W K, Heufer K A, Donohoe N, Das A K, Sung C-J, Herzler J, Naumann C, Griebel P, Mathieu O. An experimental and detailed chemical kinetic modeling study of hydrogen and syngas mixture oxidation at elevated pressures, Combust. Flame 160 (6) (2013) 995-1011.

[43] Design Reaction, CHEMKIN 10131, Reaction Des. (2013).

[44] Bartholomé E. Zur Methodik der Messung von Flammengeschwindigkeiten, Berichte der Bunsengesellschaft für physikalische Chemie 53 (4) (1949) 191-6.

[45] Koroll G, Mulpuru S. The effect of dilution with steam on the burning velocity and structure of premixed hydrogen flames, Symp. (Int.) Combust. 21 (1) (1988) 1811-9.

[46] Gelfand B E, Silnikov M V, Medvedev S P, Khomik S V.Laminar and Cellular Combustion of Hydrogenous Gaseous Mixtures. in: Thermo-Gas Dynamics of Hydrogen Combustion and Explosion, Springer; 2012, p.15-51.

[47] Edse R, Lawrence L. Detonation induction phenomena and flame propagation rates in low temperature hydrogen-oxygen mixtures, Combust. Flame 13 (5) (1969) 479-86.

[48] Kusharin A Y, Popov O, Agafonov G. Normal flame velocities in mixtures of oxyhydrogen gas with water steam, Himicheskaya Fizika 14 (4) (1995) 179-89.

[49] Kuznetsov M, Alekseev V, Matsukov I, Dorofeev S. DDT in a smooth tube filled with a hydrogen–oxygen mixture, Shock Waves 14 (3) (2005) 205-215.

[50] Gavrikov A, Bezmelnitsyn A, Leliakin A, Dorofeev S. Extraction of basic flame properties from laminar flame speed calculations, Proceedings of the 18th International Colloquium on the Dynamics of Explosions and Reactive Systems (ICDERS), (2001), paper 114.

[51] Kuznetsov M, Redlinger R, Breitung W, Grune J, Friedrich A, Ichikawa N. Laminar burning velocities of hydrogen-oxygen-steam mixtures at elevated temperatures and pressures, Proc. Combust. Inst. 33 (1) (2011) 895-903.

[52] Boivin P, Jiménez C, Sánchez A L, Williams F A. An explicit reduced mechanism for H_2–air combustion, Proc. Combust. Inst. 33 (1) (2011) 517-23.

[53] Mari R, Cuenot B, Rocchi J-P, Selle L, Duchaine F. Effect of pressure on hydrogen/oxygen coupled flame–wall interaction, Combust. Flame 168 (2016) 409-19.

[54] Lutz A E. A numerical study of thermal ignition, Report No. SAND88-8228, Sandia National Laboratories, CA, USA, 1988.

[55] Maas U, Warnatz J. Ignition processes in hydrogen-oxygen mixtures, Combust. Flame 74 (1) (1988) 53-69.

[56] Bychkov V, Akkerman V y, Fru G, Petchenko A, Eriksson L-E. Flame acceleration in the early stages of burning in tubes, Combust. Flame 150 (4) (2007) 263-76.

[57] Kerampran S, Desbordes D, Veyssière B, Bauwens L. Flame propagation in a tube from closed to open end, 39th Aerospace Sciences Meeting and Exhibit (2001), paper 1082.

[58] Massey B S. Mechanics of fluids, 6th ed. Van Nostrand Reinhold (International). US: CRC Press; 1989.

[59] Bradley D, Lawes M, Liu K, Woolley R. The quenching of premixed turbulent flames of iso-octane, methane and hydrogen at high pressures, Proc. Combust. Inst. 31 (1) (2007) 1393-400.

[60] Dong Y, Holley A T, Andac M G, Egolfopoulos F N, Davis S G, Middha P, Wang H. Extinction of premixed H_2 /air flames: chemical kinetics and molecular diffusion effects, Combust. Flame 142 (4) (2005) 374-87.

[61] Dziemińska E, Hayashi A K. Auto-ignition and DDT driven by shock wave – Boundary layer interaction in oxyhydrogen mixture, Int. J. Hydrogen Energy 38 (10) (2013) 4185-4193.

[62] Morley C. Gaseq: a chemical equilibrium program for Windows. Available from: http://www.gaseq.co.uk . (2005).

[63] Gu X, Emerson D, Bradley D. Modes of reaction front propagation from hot spots, Combust. Flame 133 (1) (2003) 63-74.

[64] Bates L, Bradley D, Paczko G, Peters N. Engine hot spots: Modes of auto-ignition and reaction propagation, Combust. Flame 166 (2016) 80-5.

[65] Bates L, Bradley D, Gorbatenko I, Tomlin A S. Computation of methane/air ignition delay and excitation times, using comprehensive and reduced chemical mechanisms and their relevance in engine autoignition, Combust. Flame 185 (2017) 105-16.

[66] Goodwin D. Cantera: Object-oriented software for reacting flows, California Institute for Technology (Caltech). Available: (accessed October, 2016) http://www.cantera.org . (2005).

[67] Short M, Sharpe G J. Pulsating instability of detonations with a two-step chain-branching reaction model: theory and numerics, Combust. Theory Model. 7 (2) (2003) 401-16.

[68] Liang Z, Browne S, Deiterding R, Shepherd J. Detonation front structure and the competition for radicals, Proc. Combust. Inst. 31 (2) (2007) 2445-53.

[69] Sirmas N, Radulescu M I. Thermal ignition revisited with two-dimensional molecular dynamics: Role of fluctuations in activated collisions, Combust. Flame 177 (2017) 79-88.